IGSHPA Research Track
Las Vegas, December 6-8, 2022

Dynamic simulation of ground source heat pump systems with non-stationary convolutions

Gabrielle Beaudry **Philippe Pasquier**

ABSTRACT

Advective processes related to groundwater motion and flow rates have a significant impact on the thermal performance of ground source heat pump systems. Including these elements during the design phase, however, remains a challenging task, as few computationally efficient modeling tools allow for their adequate and accurate representation. The present work addresses this issue by presenting the experimental validation of non-stationary convolutions for predicting the thermal response of a ground heat exchanger to both transient heat loads and advection. First, the method is outlined along with a simple demonstration case emulating the time-variation of groundwater velocity. Then, it is validated against experimental data retrieved from a 35-day multi-flow rate thermal response test conducted on a real standing column well. The results show a mean absolute error of 0.28 °C between the experimental and simulated results, which represents good accuracy considering the complexity of the thermo-hydro-processes at work. The high computing efficiency of the proposed technique is also demonstrated and suggests its potential for future implementation in common-use design tools.

INTRODUCTION

Advective processes bear a significant impact on the thermal performance of ground source heat pump systems. Groundwater motion has notably been associated with a better thermal efficiency (Fan et al. 2007, Zanchini et al. 2012, Nguyen et al. 2017), reductions of the total borehole length and lower installation costs (Capozza et al. 2013, Samson et al. 2018). Flow rate control has also shown to provide energy gains and operating costs savings in closed-loop and standing column well (SCW) systems (Zarrella et al. 2018, Beaudry et al. 2022). However, these elements are seldom considered during the design phase, partly due to modeling challenges.

Currently, the analytical solution of the moving infinite line source (MILS) allows predicting the effect of constant and steady-state groundwater flow on the temperature increment induced by a line source of heat (Sutton et al. 2003, Diao et al. 2004, Pasquier and Lamarche 2022). Consideration of more complex processes, such as transient or groundwater source heat pumps operations, usually requires using advanced and computationally intensive numerical models. Such models can be simplified through the evaluation of a transfer function representing their normalized thermal behavior, following the well-known temporal superposition theory (Claesson and Dunand 1983, Spitler and Bernier 2016). A stationary convolution product then commonly allows rapidly assessing the response to transient and dynamic heat loads, on the condition that the hydraulic conditions remain constant. This technique was recently extended to the simulation of various dynamic advective processes in ground source heat pump operations (Beaudry et al. 2021). Namely, the authors were able to reproduce the results of various simulations emulating the time-variation of circulation flow rate and groundwater velocity in a closed-loop ground heat exchanger (GHE), and the time-variation of the

Gabrielle Beaudry (gabrielle.beaudry@polymtl.ca) is a research associate and Philippe Pasquier is a professor of geological engineering at Polytechnique Montréal.

DOI: https://doi.org/10.22488/okstate.22.000032

pumping and discharge flow rates in a SCW, while reducing the computing time of several orders of magnitude compared with a reference numerical model.

The present work intends to illustrate the potential of the non-stationary convolution (NSC) technique. First, the theory behind the method is recapped along with a simple demonstration case emulating the time-variation of groundwater velocity. Then, it is for the first time validated against experimental data retrieved from a 35-day multi-flow rate thermal response test (MF-TRT) conducted on a real SCW.

NON-STATIONARY CONVOLUTIONS FOR EFFICIENT DYNAMIC SIMULATIONS

The present section summarizes an efficient simulation strategy aimed at predicting the thermal behavior of GHEs subject to dynamic heat loads as well as time-varying hydraulic conditions. The proposed strategy relies on non-stationary convolutions, a method developed in Beaudry et al. (2021) that is an extension of the well-known superposition principle to non-stationary cases. The following text details the theoretical development of the method along with a simple synthetic demonstration case and a numerical verification of the results.

Theoretical development

The temporal superposition is commonly used to evaluate the evolution of a GHE's temperature increment $\Delta T(t)$ in response to a dynamic heat load function. It is expressed as a convolution product in Eq. 1:

$$\Delta T(t) = (f * g)(t) = \sum_{j=1}^{t} f(t_j) \cdot g(t - t_{j-1}) \quad \text{with} \quad f(t_i) = q(t_i) - q(t_{i-1}) \tag{1}$$

where $f(t)$ is the incremental heat load function and $g(t)$ is the response model's transfer function. The latter represents the temperature response of a given simulation model to a normalized constant input heat load (e.g., $q(t)$=1 W/m). Eq. 1 is valid for stationary conditions, which means that all hydraulic conditions, such as groundwater velocities and circulation flow rates, must remain constant.

It has been demonstrated in recent works that the time-variation of hydraulic conditions can be considered through non-stationary convolutions (Beaudry et al. 2021, 2022). First, this method implies that the problem be defined over a simulation period using m constant time steps $t_{i=1,2,\dots,m}$. It must also be divided into s=1,2,…, n segments, each corresponding to one individual set of constant hydraulic states and represented by a different transfer function $g_{s=1,2,\dots,n}$. Note that the time indexes defining the transitions between segments are represented with $\mu_{s=1,2,\dots,n-1}$.

As a second step, the n stationary convolution products of each transfer function with the incremental heat load function $\Delta T_s(t) = (f * g_s)(t)$ are computed and combined so that the resulting function $\Delta T_{comb}(t)$ achieves the concatenation of each segment's results over their respective periods of application, such as:

$$\Delta T_{comb}(t_i) = (f * g_{s,i})(t) \tag{2}$$

where $g_{s,i}(t)$ is the transfer function relevant during segment s at time t_i. Note that this operation achieves a discontinuous transition from one convolution product to another at transition times t_{μ_s}. To represent the actual behavior of the signal following a change in hydraulic state, it is proposed to enforce a gradual transition through the evaluation and application of a scaled correction function $\lambda(t)$:

$$\lambda(t_i) = k_{s,i} \cdot \Delta T_{comb,\lambda}(t_i) \quad \text{with} \quad \Delta T_{comb,\lambda}(t_i)=(f_\lambda * g_{s,i})(t) \tag{3}$$

where $f_\lambda(t)$ is the correction incremental input function calculated from function $q(t)$ with $q(t \geq t_{\mu_s})$=0 and $k_{s,i}$ are scaling factors aimed at preserving the signal continuity over the transitions. These factors are defined for segment s at time t_i such as $k_{s,i}$=0 if t_i<t_{μ_s}, or else $k_{s,i} = \left(\Delta T_{NSC}(t_{\mu_s}) - \Delta T_s(t_{\mu_s})\right) / \lambda(t_{\mu_s})$. Lastly, the resulting correction function can then be added to obtain the final solution $\Delta T_{NSC}(t)$:

$$\Delta T_{NSC}(t) = \Delta T_{comb}(t) + \lambda(t) \tag{4}$$

Step-by-step demonstration

This section aims at demonstrating one possible application of the proposed NSC method to a simple synthetic case. The demonstration case that was selected emulates heat injection in a single borehole that would be affected by transient aquifer flow. Note that this scenario would be likely to occur during a thermal response test on a GHE located near a pumping station.

Problem definition. First, the problem is defined over a period of 7 d with m=10080 constant time steps of 1 min. The problem is also divided into n=2 segments, with the groundwater velocity set at v=1e-7 m/s during segment s=1, and at v=1.5e-6 m/s during segment s=2, the latter starting at $t_{\mu_{1=2880}}$=2 d. The dynamic heat load function $q(t)$ as well as the groundwater velocity function $v(t)$ are illustrated in Fig. 1 a) and b).

Prior to solving this dynamic problem with the NSC, an essential step is the evaluation of the transfer functions representing the system's response to a constant heat load. In the present case, the analytical expression of the MILS recently proposed by Pasquier and Lamarche (2022) was used. More precisely, the transfer functions obtained with the MILS represent the mean temperature $\Delta\bar{T}(t)$ along the borehole wall when a constant heat impulsion of q =1 W/m is applied. Note that a constant groundwater velocity of v=1e-7 m/s was considered in the case of transfer function $g_1(t)$, and v=1.5e-6 m/s in the case of $g_2(t)$. Eq. 5 presents the MILS solution of Pasquier and Lamarche (2022). The parameteric definition of the problem is detailed in Table 1 while the resulting transfer functions are shown in Fig. 1 c). Note that to simplify the demonstration, the equivalent borehole resistance is neglected.

$$\Delta\bar{T}(t) = \frac{qI_0(2\sqrt{b})}{4\pi k_g}\left(2K_0(2\sqrt{b}) - E_1(b\tau)I_0(2\sqrt{b}) - e^{-b\tau}\sum_{m=1}^{\infty}\sum_{n=0}^{\infty}\frac{b^n(m-1)!}{(-\tau)^m(m+n)!^2}\right) \text{ with } b = \left(\frac{r_b\, v_D C_w}{4k_g}\right)^2 \text{ and } \tau = \frac{4\alpha t}{r_b^2} \quad (5)$$

Table 1. Parameters used for the evaluation of the transfer functions

Parameter	Symbol	Unit	$g_1(t)$	$g_2(t)$
Borehole radius	r_b	m	0.1	0.1
Water volumetric heat capacity	C_w	MJ/(m³K)	4.20	4.20
Ground thermal conductivity	k_g	W/(mK)	2.4	2.4
Darcy velocity	v_D	m/s	1e-7	1.5e-6
Specific heat load	q	W/m	1	1
Ground volumetric heat capacity	C_g	MJ/(m³K)	1.92	1.92

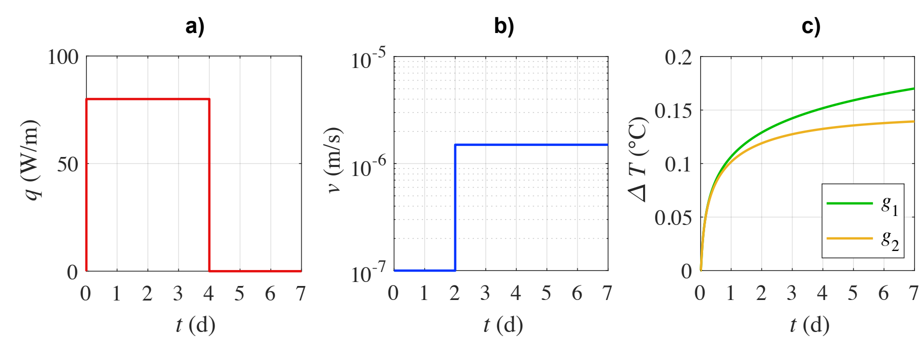

Figure 1 Definition of the demonstration case's problem representing heat injection in a single borehole with transient aquifer flow. a) heat load function, (b) groundwater velocity function, and c) corresponding transfer functions (see Table 1 for parametric description).

Solution. The steps of the NSC leading to the fast computation of the temperature response at the borehole wall following the dynamic conditions presented in Fig. 1 are illustrated in Fig. 2 below. The first step consists of a) computing the incremental heat load function $f(t)$. Then, b) the convolution products of this function with transfer functions $g_1(t)$ and $g_2(t)$, as well as their combination $\Delta T_{comb}(t)$, are evaluated. Note that the combination function achieves an abrupt transition between both convolution products at transition time t_{2880}=2 d.

To achieve a smooth transition between convolution products, the scaled correction function $\lambda(t)$ must be calculated and added to the combination results. This implies that c) the correction incremental input function $f_\lambda(t)$ is evaluated. Note that this can be done using Eq. 1, where all values following transition time t_{2880}=2 d in function $q(t)$ are replaced with zeros. Then, d) the convolution products of $f_\lambda(t)$ with both transfer functions $g_1(t)$ and $g_2(t)$, as well as their combination $\Delta T_{comb,\lambda}(t)$, are calculated. Finally, the scaling factors aiming at preserving the signal continuity are obtained, such as $k_{1,i}$=0 for t_i<t_{2880} and $k_{2,i}$=0.08 for the following times, then allowing the evaluation of the correction function $\lambda(t)$.

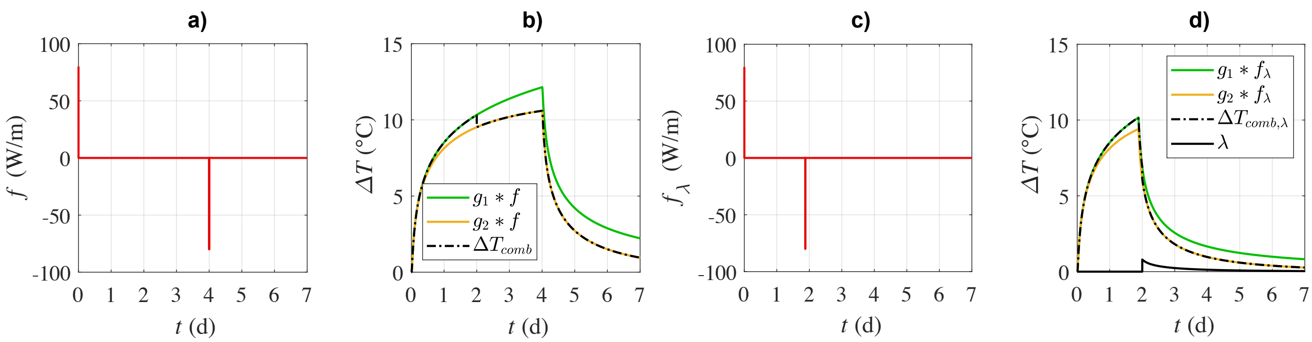

Figure 2 Step-by-step resolution of the NSC. a) incremental input function b) combination of convolution products, c) correction incremental input function, and d) combination and scaling of the correction function.

Results and numerical verification. The final solution $\Delta T_{NSC}(t)$ is presented in Fig. 3 along with convolution products $\Delta T_1(t)$ and $\Delta T_2(t)$, which represent alternative solutions that would have been obtained if the groundwater velocity stayed constant at $v(t)$=1e-7 m/s and 1.5e-6 m/s, respectively. One can appreciate the difference between the NSC solution and the constant ones, a fact that illustrates the potential impact of groundwater flow on GHEs' operations.

Fig. 3 also displays the solution of the same problem obtained with a finite-element model developed in COMSOL Multiphysics (Comsol 2022). As one can see, both signals are well superposed, which allows verifying the accuracy of the proposed NSC technique to evaluate the solution to dynamic simulations involving the time-variation of groundwater velocity. The numerical model's meshing and final solution at t=7 d are shown in Fig. 3 for the benefit of the reader. Note that the NSC calculations were achieved in 0.028 s, compared to 38 min for the numerical simulation using the same 1-min time step.

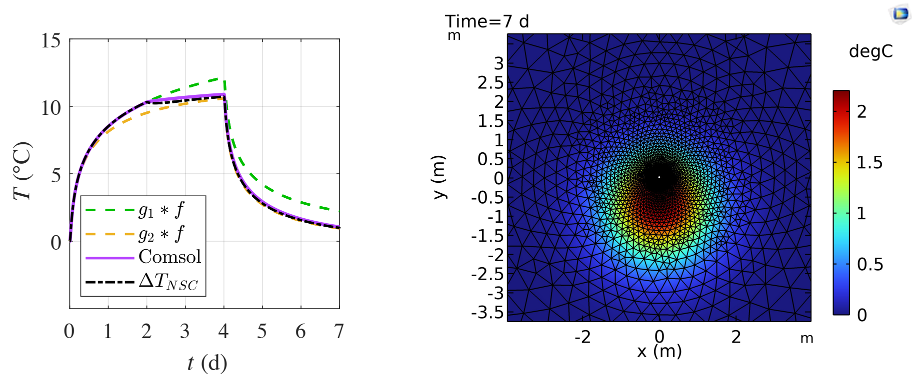

Figure 3 Numerical verification of the solution provided by the NSC for the synthetic test case emulating heat injection in a single borehole with transient aquifer flow. Comparison of the NSC and numerical final solutions (left), and close-up of the numerical model emulating a line-source of heat at t =7 d (right).

EXPERIMENTAL VALIDATION

In the previous section, the NSC method was applied to a simple case emulating the temperature response of a GHE to time-varying heat loads and groundwater flow. It should be noted that the NSC allows considering various other dynamic advective heat transfer processes, namely fluid circulation flow rates in closed-loop systems, and pumping and discharge flow rates in SCWs (Beaudry et al. 2021).

To demonstrate the accuracy as well as the large application range of the NSC, the following section presents an experimental validation of this method that relies on data acquired during a MF-TRT performed on a real SCW in 2019.

Data acquisition

Description of the experimental setup. The experimental site is located near Montreal, Canada. A 215-m-deep SCW (⌀ 165 mm) is connected to a mobile geothermal laboratory assembled in a 12.2-m marine container and equipped with, among other equipment, a 24-kW water heater and a comprehensive data control and acquisition system (see Fig. 4). See Beaudry et al. (2019), Nguyen et al. (2020), and Cerclet et al. (2020) for further details about this installation.

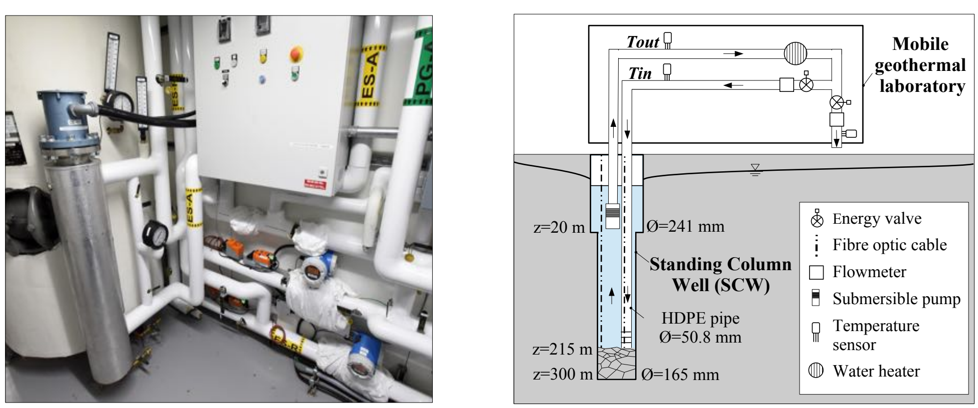

Figure 4 Simplified experimental apparatus used for the MF-TRT. Photo of the water heater and flowmeters inside the geothermal laboratory (left) and schematic view of the SCW and mechanical equipment (right).

Multi-flow rate thermal response test. Between June 3rd and July 9th, 2019, a 35-day MF-TRT was conducted on the experimental SCW to evaluate the influence of pumping and discharge flow rates on the thermal behavior of the system. Prior to the test, a temperature profile was measured in the SCW using a downhole temperature sensing system (see Fig. 5 a). Following a 2-day recirculation phase, four subsequent heating-restitution cycles were then achieved using the 24-kW water heater. The heat load (Q) imposed to the SCW was verified with the energy balance equation and is presented in Fig. 5 b). Note that the power consumption of the submersible pump (1.4 kW) and the high air temperature during the test (around 20 °C outside and 30 °C inside the laboratory) were considered as heat contamination sources. The pumping ($\dot{V}$) and discharge ($\dot{B}$) flow rates were also monitored during the test and are presented in Fig. 5 c) and d).

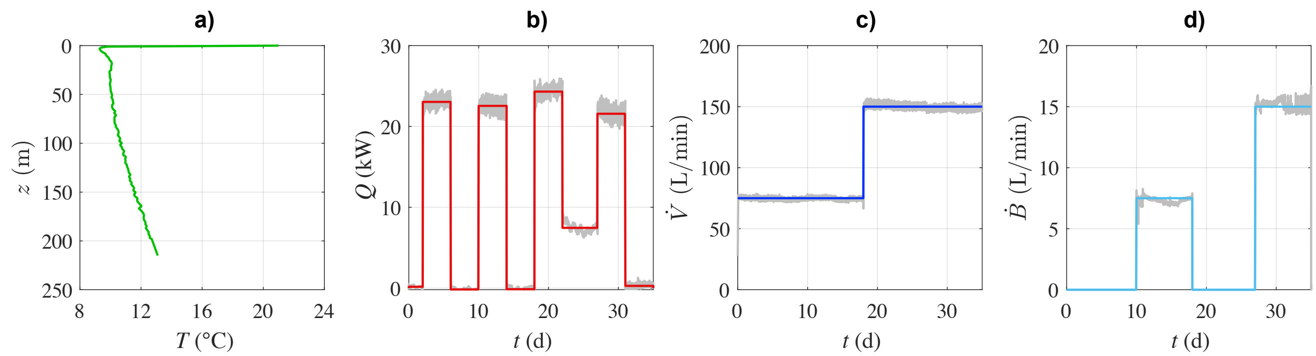

Figure 5 Experimental data acquired during the MF-TRT. a) temperature profile measured in the annular space of the SCW prior to the test, b) heating load applied to the groundwater loop, c) pumping flow rate, and d) discharge flow rate during the test. The minutely data is presented in grey, and the average step-value is colored.

Modeling particularities

The NSC method was used to predict the evolution of the temperature at the outlet of the well $T_{out}(t)$ in response to the heat load and flow rate functions shown in Fig. 5. The methodology is the same that was presented earlier, except for the nature of the response model used in the evaluation of the transfer functions, and for the consideration of the non-uniform temperature profile.

Numerical transfer functions. The thermal behavior of SCWs is highly influenced by the coupled processes of heat transfer and groundwater flow, both in the aquifer and inside the well. Thus, a high-precision finite-element model coupling heat transfer to Darcian groundwater flow was employed as a response model. Note that the model was built to emulate the experimental SCW system and was validated against experimental data in Beaudry et al. (2019). The numerical model was first used to evaluate the transfer functions g_s representing the normalized response of the SCW to a constant heat load of 1 kW (see Fig. 6), a method that was used and described in previous works (Pasquier and Marcotte 2014, Nguyen et al. 2017, Beaudry et al. 2021). To this end, the model was solved four times, that is one time for each different set of constant flow rates corresponding to the MF-TRT.

Non-uniform thermal boundary condition. The mean ground temperature along borehole depth T_0 is often added to the temperature increment calculated in the convolution process to obtain the final solution. To account for the the combined effect of the non-uniform hydraulic conductivity and temperature profile, a second set of transfer functions h_s was rather evaluated in the present case (see Fig. 6), as proposed for stationary cases in Nguyen et al. (2017). The NSC was then performed using these transfer functions and a unitary input to obtain a time-varying function $T_0(t)$.

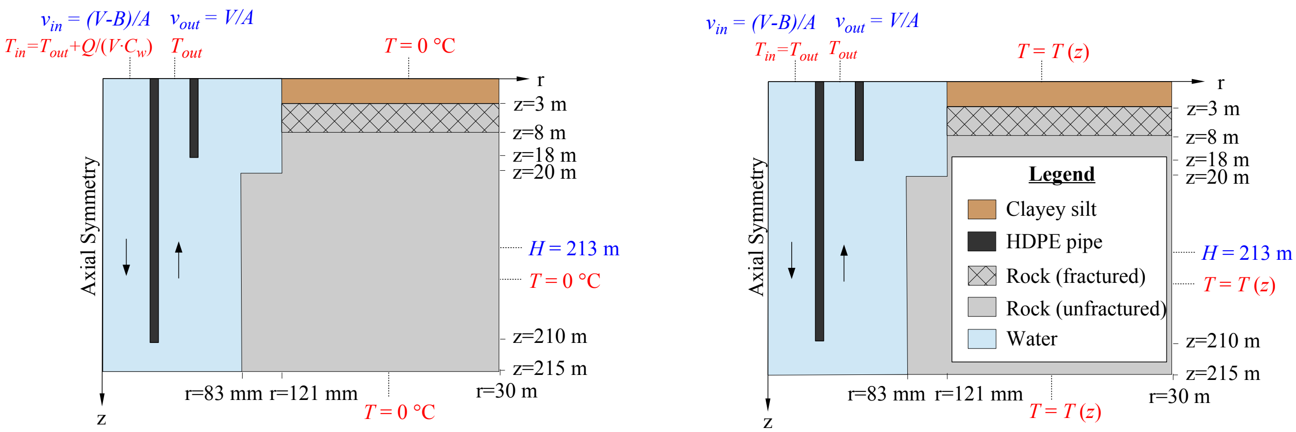

Figure 6 Geometry, hydraulic (blue) and thermal (red) boundary conditions of the numerical model coupling heat transfer to Darcian groundwater flow. Definition for the evaluation of transfer functions g_s with uniform thermal boundary conditions (left) and h_s with non-uniform thermal boundary conditions (right). Adapted from Beaudry et al. (2019).

Results

The results of the experimental validation are presented in Fig. 7. Fig. 7 a) first displays the temperature increment of the groundwater at the outlet of the well in response to the heating loads and operating flow rates that was calculated with the NSC. In Fig. 7 b), the response of the system to the non-uniform temperature profile and operating flow rates is shown. At last, Fig. 7 c) illustrates the superposition of the NSC final solution with the experimental results. Both signals display the same behavior, and a mean absolute error (MAE) of 0.28 °C is calculated, which demonstrates the accuracy of the NSC method for predicting the temperature response of a GHE to time-varying heat loads and operating flow rates. Note that Figure 7 c) also compares the outlet fluid temperature that would have been obtained using a stationary convolution with a constant circulation flow rate of $\dot{V}$=75 L/min, a constant discharge flow rate of $\dot{B}$=0 L/min and a uniform inital ground temperature of 11 °C. From Figure 7 c), it is clear that the NSC can not only accurately reproduce the experimental measurements but can also take into account the dynamic operation of the GHE, a feature that stationary convolution can visibly not integrate accurately over a long simulation period of 35 days.

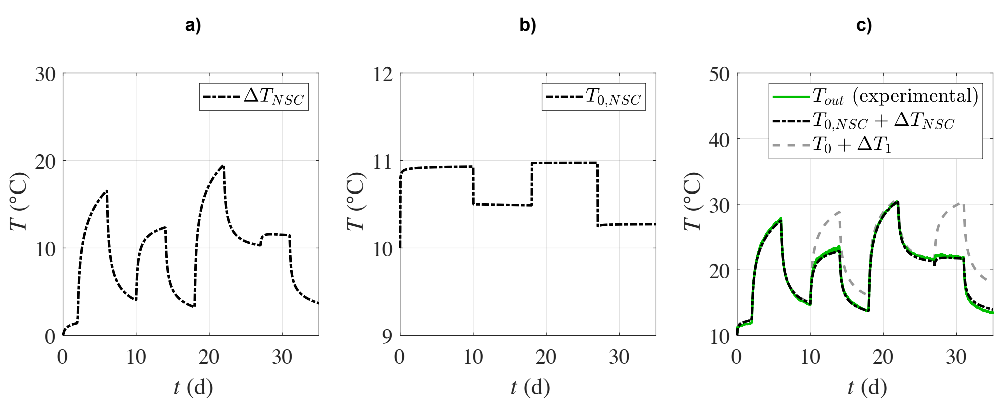

Figure 7 Experimental validation of the NSC against a multi-flow rate thermal response test. a) temperature increment at the borehole's outlet calculated with the NSC, b) temperature at the borehole's outlet considering the non-uniform temperature profile and c) superposition of the NSC with the experimental results (MAE=0.28 °C), and comparison with a stationary solution.

Finally, note that the whole convolution process took 9.5 s while the simulation time required to obtain the four transfer functions is around 80 min. By comparison, a fully dynamic numerical simulation with the finite-element method using the same 1-min time step lasted for approximately 26 h. For the moment, the main limitation to the use of NSC is the effort required to obtain numerically the various transfer functions. Additional works based on the use of artificial neural networks to obtain instantly the transfer function of closed-loop GHEs (Pasquier et al. 2018, Dusseault and Pasquier 2019) or of SCWs (Jacques and Pasquier 2022a, 2022b) are already undergoing and should ease this constraint.

CONCLUSIONS

Previous numerical verifications have shown the robustness and accuracy of non-stationary convolutions for dynamic simulation, including for transient circulation flow rates in closed-loop GHEs, and for transient circulation and discharge flow rates in SCWs. In this work, the potential of non-stationary convolutions has been illustrated with a simple analytical problem as well as with a real thermal response test lasting 35 days. The results show the ability of non-stationary convolutions to reproduce analytical and experimental temperature responses. The high computational efficiency of the proposed technique is also demonstrated and suggests its potential for future use in mainstream design tools.

ACKNOWLEDGMENTS

The authors acknowledge the support from partners of the Geothermal Research Chair on the Integration of SCWs in Institutional Buildings, namely Hydro-Québec, the Ministry of Higher Education of Québec, CSSMI, CSSDM, CSSS, Versa Profiles, Marmott Energy, CanmetEnergy and NSERC. This work was financed by the Natural Sciences and Engineering Research Council of Canada through grant number ALLRP 544477-19.

NOMENCLATURE

α = Thermal diffusivity (m^2/s)
A = Area (m^2)
$\dot{B}$ = Discharge flow rate (m^3/s)
C = Volumetric heat capacity ($J/m^3{\cdot}K$)
k = Thermal conductivity ($W/m{\cdot}K$)
q = Specific heat load (W/m)
Q = Heat load (W)
r = Radial distance from the line source (m)
t = Time (s)
T = Temperature (°C)
$\dot{V}$ = Pumping flow rate (m^3/s)
v_D = Darcy velocity (m/s)

Subscripts

b = borehole
w = water
g = ground
o = initial

REFERENCES

Beaudry, G., Pasquier, P., Marcotte, D., 2021. A fast convolution-based method to simulate time-varying flow rates in closed-loop and standing column well ground heat exchangers. Renewable Energy 174, 55–72.

Beaudry, G., Pasquier, P., Marcotte, D., 2019. The impact of rock fracturing and pump intake location on the thermal recovery of a standing column well: model development, experimental validation, and numerical analysis. Science and Technology for the Built Environment 25, 1052–1068.

Beaudry, G., Pasquier, P., Marcotte, D., Zarrella, A., 2022. Flow rate control in standing column wells: A flexible solution for reducing the energy use and peak power demand of the built environment. Applied Energy 313, 118774.

Capozza, A., De Carli, M., Zarrella, A., 2013. Investigations on the influence of aquifers on the ground temperature in ground-source heat pump operation. Applied Energy 107, 350–363.

Cerclet, L., Courcelles, B., Pasquier, P., 2020. Impact of standing column well operation on carbonate scaling. Water 12.

Claesson, J., Dunand, A., 1983. Heat extraction from ground by horizontal pipes. Swedish Council of building Research, Swedish Council for Building Research. ed. Stokholm.

Comsol Multiphysics, 2022. COMSOL, Version 5.5. Burlington, MA, USA.

Diao, N., Li, Q., Fang, Z., 2004. Heat transfer in ground heat exchangers with groundwater advection. International Journal of Thermal Sciences 43, 1203–1211.

Dusseault, B., Pasquier, P., 2019. Efficient g-function approximation with artificial neural networks for a varying number of boreholes on a regular or irregular layout. Science and Technology for the Built Environment 25, 1023–1035.

Fan, R., Jiang, Y., Yao, Y., Shiming, D., Ma, Z., 2007. A study on the performance of a geothermal heat exchanger under coupled heat conduction and groundwater advection. Energy 32, 2199–2209.

Jacques, L., Pasquier, P., 2022a. Interpretation of a thermal response test in a Bayesian framework to infer the hydraulic properties surrounding a standing column well. Presented at the EGU General Assembly 2022, Vienna, Austria.

Jacques, L., Pasquier, P., 2022b. Uncertainty assessment of the hydraulic properties surrounding a standing column well with a thermal response test. IGSHPA Research Track 2022, Las Vegas., United States. Currently under review.

Nguyen, A., Beaudry, G., Pasquier, P., 2020. Experimental assessment of a standing column well performance in cold climates. Energy and Buildings 226, 110391.

Nguyen, A., Pasquier, P., Marcotte, D., 2017. Borehole thermal energy storage systems under the influence of groundwater flow and time-varying surface temperature. Geothermics 66, 110–118.

Pasquier, P., Lamarche, L., 2022. Analytic expressions for the moving infinite line source model. Geothermics 103, 102413.

Pasquier, P., Zarella, A., Labib, R., 2018. Application of artificial neural networks to near-instant construction of short-term g-functions. Applied Thermal Engineering 143, 910–921.

Pasquier, P., Marcotte, D., 2014. Joint use of quasi-3D response model and spectral method to simulate borehole heat exchanger. Geothermics 51, 281–299.

Samson, M., 2018. Influence of groundwater flow on cost minimization of ground coupled heat pump systems. Geothermics 73, 100–110.

Spitler, J.D., Bernier, M., 2016. Vertical borehole ground heat exchanger design methods, in: Advances in Ground-Source Heat Pump Systems. Elsevier, pp. 29–61.

Sutton, M.G., Nutter, D.W., Couvillion, R.J., 2003. A ground resistance for vertical bore heat exchangers with groundwater flow. Journal of Energy Resources Technology 125, 183–189.

Zanchini, E., 2012. Long-term performance of large borehole heat exchanger fields with unbalanced seasonal loads and groundwater flow. Energy 38, 66–77.

Zarrella, A., Emmi, G., De Carli, M., 2017. A simulation-based analysis of variable flow pumping in ground source heat pump systems with different types of borehole heat exchangers: A case study. Energy Conversion and Management 131, 135–150.